Biophysical Chemistry 149 (2010) 92–101

Contents lists available at ScienceDirect

Biophysical Chemistry

journal homepage: http://www.elsevier.com/locate/biophyschem

Structure and conformational studies on dityrosine formation in the DNA binding domain of RFX5

Madhumita Chakraborty [a], Dipankar Bhattacharya [a], Chaitali Mukhopadhyay [b], Abhijit Chakrabarti [a,*]

[a] Biophysics Division and Structural Genomics Section, Saha Institute of Nuclear Physics, 1/AF, Bidhannagar, Kolkata 700064, India
[b] Department of Chemistry, University of Calcutta, Kolkata 700009, India

ARTICLE INFO

Article history:
Received 18 March 2010
Received in revised form 17 April 2010
Accepted 18 April 2010
Available online 24 April 2010

Keywords:
DNA binding domain of RFX5
Dityrosine
Fluorescence
X-box DNA
UV oxidation

ABSTRACT

The DNA binding protein RFX5 is a subunit of RFX complex involved in transcription regulation of MHCII molecules. The RFX complex binds to the X-box DNA through the DNA binding domain of RFX5. We have examined the formation of intramolecular tyrosine cross linking, dityrosine, in RFX5DBD under oxidative stress, through UV irradiation and enzymatic action of H_2O_2/peroxidase by fluorescence spectroscopic studies. Dityrosine (DT) was formed predominantly in alkaline condition showing its intense characteristic fluorescence emission. Homology modeling indicated Y^{39} and Y^{42} could be the potential tyrosine residues undergoing oxidative cross-linking. Conformational changes in RFX5DBD under oxidative stress were observed by CD measurements. The *in vitro* association of X-box DNA with RFX5DBD increased DT fluorescence significantly and protected RFX5DBD from UV irradiation as observed in SDS-PAGE followed by mass spectrometric analysis. Results indicate cross protection in both RFX5DBD and DNA under oxidative stress playing important role in protein modification.

1. Introduction

Oxidative modification of proteins under oxidative stress is a well known phenomenon in biological system [1–4]. The principle of oxidative modification of proteins due to the exposure of ionizing radiation is widely studied [5,6]. Under the influence of ionizing radiation reactive oxygen species (ROS) are generated which are mainly hydroxyl radical (OH•) and super oxide anion radical ($O_2^{-\bullet}$). They not only oxidize protein backbone resulting in protein fragmentation but also trigger side chain modification through intra- or inter-molecular protein–protein cross-linkage [7]. Modification in protein occurs most readily to the side chains of amino acid residues Cys, Met, Trp, Tyr, His and Phe [8]. The two major intrinsic fluorophores in protein are tryptophan and tyrosine. The tryptophan oxidation products are kynurenine and N-formyl kynurenine. Kynurenine, a weak fluorescence emitter, has emission maxima in the region of 490–525 nm. N-formyl kynurenine (NFK) has strong emission at around 434 nm [9–11]. One of the common tyrosine side chain modifications is the formation of dityrosine (DT) [12–14]. DT cross-links in proteins take place due to the coupling of two Tyr• generated by OH• which snatches one H atom from the phenolic ring of the Tyr residue. The steps involved in dityrosine formation are radical isomerization, di-radical reaction and finally enolization [15]. DT formation has been schematically shown in Fig. 1 [16]. DT formation is also initiated by photo ejection of electron upon UV irradiation, catalyzed by peroxidase and is facilitated under alkaline pH [17–21]. It is a good marker for protein modification, detectable by its emission maxima at 400 nm upon excitation at 315–320 nm [15–17] and is distinguished from another tyrosine oxidized product dihydroxyphenylalanine (DOPA) which emits at 315 nm upon excitation at 280 nm [22]. However Huggins et al. have reported the formation of some uncharacterized DT like fluorescent products in lysozyme and RNase along with DT whose contribution depended on protein, type of oxidation and extent of oxidative damage [23]. Reducing agents like DTT and glutathione inhibit DT formation [24,25]. We have investigated the formation of DT in the DNA binding domain (DBD) of the regulatory factor X5 (RFX5) protein in the presence and absence of X-box DNA.

RFX5 (75 kDa) is the largest subunit of a multimeric DNA binding complex called RFX. Two other subunits are RFXAP (45 kDa) and RFXANK (35 kDa). RFX is one of the major components in the regulation and expression of major histocompatibility complex (MHC) class II gene which is present in antigen presenting cells and presents antigenic peptides to $CD4^+$ T cells [26–29]. RFX binds to the X-box sequence in upstream of the promoter of MHCII gene and

Abbreviations: MHC, Major histocompatibility complex; RFX, Regulatory factor X; RFX5DBD, N-terminal DNA binding domain of RFX5; DT, Dityrosine; DTT, Dithiothrietol; HRP, Horseradish peroxidase; UV, Electromagnetic radiation in the ultraviolet region; λ_{max}, Wavelength of maximum fluorescence emission; SDS-PAGE, SDS polyacrylamide gel electrophoresis; SEM, Standard error of the mean; IPTG, Isopropyl β-D-1 thiogalactopyranoside; PMSF, Phenyl methyl sulfonyl fluoride; GST, Glutathione S-transferase; CHCA, α-cyano-4-hydroxycinnamic acid.

* Corresponding author. Tel.: +91 33 2337 5345 49; fax: +91 33 2337 4637.
E-mail address: abhijit.chakrabarti@saha.ac.in (A. Chakrabarti).

0301-4622/$ – see front matter © 2010 Elsevier B.V. All rights reserved.
doi:10.1016/j.bpc.2010.04.005

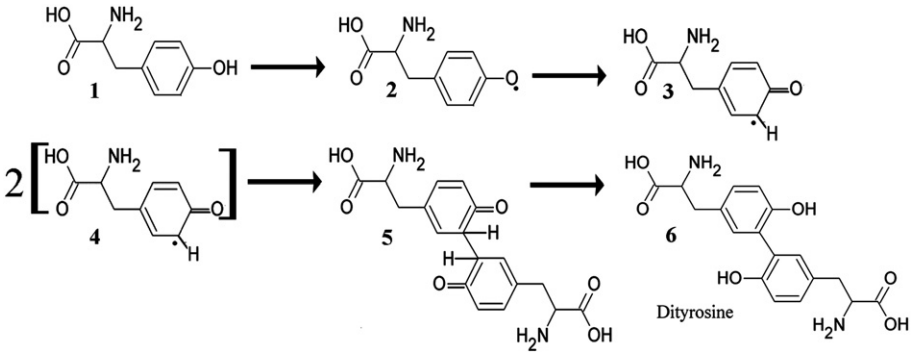

Fig. 1. Scheme of formation of dityrosine. (1) Tyrosine, (2) tyrosine radical formation by UV treatment, (3) radical isomerization, (4) two radicals combined, (5) radical recombination and (6) dityrosine formation.

nucleates the formation of MHC II enhanceosome in which a number other proteins namely cyclic AMP response element binding (CREB) protein, nuclear factor Y (NF-Y) and class II transcriptional activator (CIITA) are present [30–35]. RFX5 is the fifth member of a family of mammalian DNA binding protein where the DBD is highly conserved in all the proteins belonging to this family [36]. It is well known that reactive oxygen species are generated within antigen presenting cells as a byproduct of mitochondrial electron transport. In addition NADPH oxidase holoenzyme induces the production of high level of superoxide anion which generates reactive oxygen species (ROS) when converted to hydrogen peroxide [37]. Increased ROS level enhance the class II expression as a result of increased DNA binding ability of NF-Y [37,38] which binds Y box in the upstream of promoter region of MHC II. As the Y box binding protein has been found to be redox sensitive, the effect of oxidative stress on X-box binding protein or more specifically the DNA binding factor, RFX5DBD has been investigated. We have studied the overall conformation of RFX5DBD under oxidative stress and have identified modification of amino acid side chains in RFX5DBD, for the first time, using a combination of fluorescence spectroscopy, CD and mass spectrometry. The protein has been cloned, expressed and purified and the intrinsic fluorescence studies revealed facile formation of intra molecular DT derivatives *in vitro*, more significantly under alkaline condition. From homology modeling of the protein we found that the core Y^{39} and Y^{42} are spatially in close proximity and are in more suitable position to form DT than the other pairs of tyrosine residues (between Y^{42}–Y^{45} and Y^{14}–Y^{18}). Borate quenches DT formation in RFX5DBD where as H_2O_2/peroxidase treatment enhances it [17,39]. Circular dichroism (CD) analysis of the protein before and after formation of DT, as detected from its characteristic fluorescence emission at ~400 nm, indicated alteration of the secondary structure of the protein under alkaline condition at pH 11 when DT formation is facilitated. The presence of X-box DNA significantly increased the intensity of DT fluorescence. Formation of DT in RFX5DBD followed pseudo first order kinetics with enhancement in the rate of formation of DT in presence of X-box DNA. We have also investigated the changes in RFX5DBD under UV stress in presence and absence of DNA. SDS-PAGE analysis showed that DNA protected RFX5DBD from UV induced oxidative damage. We have also identified the peptide sequence in the protein, prevented from oxidation, using MALDI ToF/ToF tandem mass spectrometry which was in conformity with what we obtained from the homology modeling studies.

2. Materials and methods

2.1. Materials

Deep $Vent_R$ Taq DNA polymerase and all restriction enzymes were purchased from New England Biolabs (MA, USA). Superdex™-75 10/300 GL size exclusion column, pGEX vectors, Glutathione-Sepharose™ 4 Fast Flow, Hybond-N+ positively charged nylon membrane (0.45 μm) were obtained from GE Healthcare, Biosciences AB (Sweden). Complete protease inhibitor cocktail was from Roche (Mannheim, Germany). Restriction grade thrombin was obtained from Novagen (Madison, WI). Ampicillin, IPTG and HRP, Type VI-A (1000 units/mg), CHCA matrix, acetonitrile, TFA were purchased from Sigma-Aldrich (St. Louis, MO). Sequencing grade trypsin was obtained from Promega (Madison, WI). Biotin 3′ End DNA Labeling Kit, LightShift® chemiluminescent EMSA Kit, Chemiluminescent Nucleic Acid Detection Module were purchased from Pierce (Rockford, IL).All other chemicals were of analytical grade and were purchased locally. Milli|Q grade water (Sartorious UF 116) or quartz distilled water was used for the preparation of buffers and all other solutions.

2.1.1. Cloning of RFX5DBD

The human RFX5 cDNA was generously given by Dr. Jenny P.Y. Ting, (UNC Lineberger Comprehensive Cancer Centre, University of North Carolina). The DNA binding domain of RFX5 (76–158 amino acids) was selected using SMART (ExPassy protparam tool). Human RFX5 cDNA was used as templates for PCR amplification using the Expand High Fidelity PCR system kit along with Deep $Vent_R$ Taq DNA polymerase. The primer used to amplify the cDNAs encoding the DNA binding domain of RFX5 is mentioned below. The amplification conditions for RFX5DBD were, 5 min at 95 °C, followed by 4 cycles of 1 min at 95 °C, 1 min at 58 °C, 1 min at 72 °C then 24 cycles of 1 min at 95 °C, 1 min at 65 °C, 1 min at 72 °C and finally 7 min at 72 °C. PCR amplified DNA was digested with ECoRI/XhoI restriction enzymes and then was inserted at ECoRI/XhoI sites into pGEX-4 T1. The authenticity of the construct was verified by DNA sequencing.

RFX5DBD-(F) (29mer) 5′ CCGGAATTCGGAGACAAAAGCTCAGAGCC 3′.

RFX5DBD-(R) (32mer) 5′ CCGCTCGAGTCAGCCACTGTAGCAA-TATTTGG 3′.

2.1.2. Expression and purification of RFX5DBD

To express the recombinant RFX5DBD, competent *Escherichia coli* BL21 cells were transformed with pGEX-4 T1 with cDNA encoding RFX5DBD. Transformed cells were grown in 2 liter LB medium at 37 °C supplemented with 100 μg/ml ampicillin. After the cell density reached 0.8 OD_{600nm} IPTG at a final concentration of 0.9 mM was added to induce the production of recombinant RFX5DBD at 20 °C. After overnight induction the cells were collected by centrifugation. Bacterial cell pellets were resuspended in 15 ml of lysis buffer (20 mM Tris–HCl pH 8.0, 200 mM NaCl, 5% glycerol) supplemented with complete protease inhibitor cocktail. Cells were lysed by sonication in ice and subsequent freeze thawing. Lysates were spun at 18,000 × *g* for 30 min at 4 °C. Pre-equilibrated Glutathione-Sepharose 4B beads were added to the supernatants (3 ml packed bead for 2 liter cultured medium) and treated on a rotary shaker for 2 h at 4 °C. It was then spun for 5 min at 600 × *g* and the supernatant was removed with the

GST fused protein remained attach to the beads. Beads were washed extensively with the lysis buffer to remove the non-specifically bound proteins and were then incubated overnight at 4 °C with restriction grade thrombin for in-bead digestion of the proteins. After collecting GST free RFX5DBD, reaction was quenched with PMSF (0.2 mg/ml). Further purity was achieved by HPLC (Unicorn Acta, GE Healthcare, Sweden) using superdex™-75 10/300 GL size exclusion column. The column buffer contained 10 mM sodium phosphate, 150 mM NaCl, pH 7.5. The protein was concentrated using an Amicon ultra 5-kDa spun column (Millipore, Bedford, MA, USA) and stored at 4 °C for less than 7 days.

2.1.3. Preparation of double stranded X-box DNA

The double stranded X-box DNA was prepared by dissolving the high purity single stranded oligonucleotides in 10 mM Tris–HCl at pH 8, 1 mM EDTA and 80 mM NaCl, mixing the complementary strands in equimolar amounts and then heated at 95 °C for 5 min and slowly cooled to room temperature. The purity was checked by gel electrophoresis. The X-box sequence is as follows: (F), 5′-CCCCCCCTTCCCCTAGCAACAGATGCGT-CATC-3′ (R), 5′-GATGACGCATCTGTTGCTAGGGGAAGGGGGGG-3′.

2.1.4. Electrophoretic mobility shift assay

EMSA, for protein–DNA interaction, was performed with X-box DNA sequence and was detected by chemiluminescent method. For this purpose complementary oligos were labeled separately with 1–3 biotinylated ribonucleotides onto the 3′ end of DNA strands using terminal deoxynucleotidyl transferase according to the manufacturer's instructions. Annealing was done by mixing equal amounts of the labeled complementary oligos and denaturing it at 90 °C for 1 min and then slowly cooling at room temperature. Binding buffer for EMSA contained 10 mM Tris pH 7.5, 50 mM KCl, 1 mM DTT, 2.5% glycerol, 5 mM $MgCl_2$, 0.05% NP-40, 50 ng/μl Poly(dI-dC) as non-specific competitor DNA. The reaction mixture contained equal amount of biotinylated DNA and 5 μM RFX5DBD in all sets. The reaction was allowed to proceed for 30 min at room temperature and finally quenched with 5× loading buffer. Samples were run in a 6% non-denaturing mini polyacrylamide gel using 0.5× TBE buffer for 1.5 h at 100 V in a cooled atmosphere. Gel was then transferred to hybond-N+ positively charged nylon membrane at 380 mA for 1 h. The transferred DNA was then cross-linked to the membrane using GS Gene Linker® UV Chamber (Bio Rad Herculis, CA) equipped with 254 nm bulbs with energy of 120 mJ/cm^2 for 60 s. Biotinylated DNA was then detected by chemiluminescence method using "Chemiluminescent Nucleic Acid Detection Module" as per instruction of the manufacturer. A control experiment was performed by treating biotinylated X-box DNA with 5 μM BSA where all other steps were exactly similar.

2.2. Fluorescence characterization of DT at various pHs

Steady state fluorescence spectra were recorded on Fluoromax-3 spectrofluorometer (Jovin Yvon Horiba, Edison, NJ). Fluorescence emissions from tyrosine and DT were measured using excitation at 280 and 315 nm respectively. Slits with bandwidths of 5 nm were used both for excitation and emission channels. Compositions of the buffers used at various pHs were acetic acid-sodium acetate pH 5, Mes-sodium hydroxide pH 6, phosphate buffer pHs 7 and 7.5, Tris–HCl pHs 8 and 8.5 and glycine-sodium hydroxide pHs 9, 9.5, 10, 10.5, 11, and 11.5 respectively. For all pH titrations 0.03 mg/ml of protein was incubated with the respective buffers containing 150 mM NaCl, for 10 min on ice before recording each emission spectrum. Control baselines were subtracted for each spectrum in all fluorescence measurements. All fluorescence experiments were performed at different pH in presence and absence of 100 mM DTT to study the formation of DT in RFX5DBD.

UV irradiation of RFX5DBD for the formation of DT was done in the fluorescence spectrometer for 5 min using the excitation wavelength at 280 nm and the excitation bandwidth kept at 10 nm. Similar procedure was followed in presence of equimolar pre incubated X-box DNA with 15 min incubation time prior to UV irradiation. The rate constants for DT formation in RFX5DBD with and without DNA were determined non-linear curve fitting method using Origin 7.5.

2.3. H_2O_2/peroxidase catalyzed DT formation

The peroxidase catalyzed reaction mixture contained 5 μg/ml of HRP, 0.03 mg/ml of RFX5DBD in 40 mM glycine-sodium hydroxide pH 11, in presence of 1 mM H_2O_2 [19].

2.4. Quenching of DT by borate/boric acid

0.03 mg/ml of RFX5DBD was incubated with 0.5 M sodium monoborate-boric acid buffer at pH 8.7 for 10 min on ice and DT formation was monitored by fluorescence measurements at ~400 nm upon excitation at 315 nm.

2.5. Circular dichroism measurement

CD spectra were recorded on a CD spectrometer of BioLogic Science Instruments (France) using a rectangular quartz cell of path length of 0.1 mm. Measurements were taken at wavelengths between 190 nm and 250 nm at a scan rate of 3 nm/min. A total of three scans were averaged to obtain each spectrum and they were baseline subtracted for buffer. 15 μM of RFX5DBD was taken for each measurement at pHs 7.5 and 11 in presence and absence of HRP/H_2O_2 treatment as described above. The percentage of helicity was estimated following standard protocol [40].

$$\text{Percentage of helicity} = 100 \times \left({}^{\text{cal}}[\theta]_{222} / {}^{\max}[\theta]_{222}\right) \quad (1)$$

where ${}^{\max}[\theta]_{222}$ stands for 100% helicity and is calculated using the formula

$${}^{\max}[\theta]_{222} = -40{,}000 \times [1-(2.5/n)] \quad (2)$$

where n is the total number of amino acid residues in the protein and $[\theta]_{222}$ is the mean residue molar ellipticity in degrees cm^2 dmol^{-1}. ${}^{\text{cal}}[\theta]_{222}$ is obtained with the help of the following equation

$${}^{\text{cal}}[\theta]_{222} = (100 M_r \theta) / (clN_A) \quad (3)$$

θ is the experimental ellipticities in degrees, M_r is the molecular mass of the protein in Da, c is the concentration of the protein in milligram per milliliter, l is the pathlength in centimeters, and N_A is the number of residues in protein.

Quantitative estimation of the secondary structure of the protein under different conditions from the far UV-CD spectra were made by CDSSTR using CDPro analysis software, "A Software Package for Analyzing Protein CD Spectra" (http://lamar.colostate.edu/~sreeram/CDPro/main.html).

2.6. Lifetime measurement of DT in RFX5DBD

Fluorescence lifetime was measured using a time-domain fluorescence spectrometer assembled in the laboratory with components from Edinburgh Analytical Instruments (EIA, U.K.) and EG and G ORTEC (U.S.A) and operated in the time-correlated single photon counting mode. Excitation was provided by a pulsed high pressure 1.5 atm N_2 lamp. 0.175 mg/ml of RFX5DBD at pH 11 was UV irradiated and steady state fluorescence spectra were taken to confirm DT

formation prior to lifetime measurement of the DT fluorophore. The DT of RFX5DBD was excited at 315 nm and the emission decay profile was monitored at 400 nm for DT. The time resolved measurements were performed collecting 3500 photon counts in the peak channel. Intensity decay curve was fitted to a bi-exponential series and details of the mean lifetime determinations are elaborated in our earlier works [41,42].

2.7. Homology modeling of RFX5DBD

Homologous protein for RFX5DBD is RFX1DBD (source organism for both proteins is *Homo sapiens*) whose crystal structure is known. The sequence identity and similarity between these two proteins as obtained from psi blast are 33% and 60% respectively. Secondary structure of RFX5DBD was predicted using 'Phyre' version 0.2, (http://www.sbg.bio.ic.ac.uk/phyre/). Homology model of RFX5DBD was built using Modweb (http://modbase.compbio.ucsf.edu/ModWeb20-html/modweb.html). Sequence was submitted with the default settings of the program. No template was provided so that the program could search most appropriate template from Protein Data Bank. The model was built from amino acid sequence 19 to 83 of RFX5DBD based on the sequence homology with RFX1DBD (PDB code 1DP7). First few amino acids of RFX5DBD, from 11 to 18 were added to the rest of the model with the help of Insight II software (98.0 version, Accelrys Inc., running on a Silicon Graphics O_2 workstation) as a continuity of the first helix and energy minimization was performed in Insight II. The molecule was visualized and analyzed in VMD-XPLOR software package [43] running on window.

2.8. DT formation in RFX5DBD in presence of X-box DNA

Equimolar mixture of RFX5DBD and X-box DNA (2.5 μM each) were incubated at 4 °C for 30 min at two different pHs, 7.5 and 11 respectively, before recording emission spectra.

2.9. Oxidative damage of RFX5DBD in presence and absence of X-box DNA

RFX5DBD (20 μM) was treated with 1 mM H_2O_2 and 5 μg/ml of HRP at 25 °C for 15 min and then exposed to UV radiation at 254 nm for bursts of 10 and 25 s respectively using GS Gene Linker® UV Chamber (Bio Rad Herculis, CA). Similar treatment was done in presence of X-box DNA while the protein was pre-incubated with equimolar concentration of the target DNA for 10 min prior to oxidative treatment. Samples were then loaded onto 15% SDS-PAGE gel and densitometric analysis of the bands was performed on a Versa Doc series 3000 imaging system using Quantity One software (version 7.1, BioRad).

2.10. In-gel tryptic digestion and MALDI mass spectrometry

Gel spots from Coomassie stained 1D gels were digested with trypsin and mass spectrometry was performed following our earlier work [44]. Briefly, the gel pieces were destained with 50% acetonitrile in 25 mM ammonium bicarbonate followed by reduction and alkylation. In gel tryptic digestion was performed using sequencing grade trypsin overnight. The eluted peptides were analyzed in a MALDI ToF/ToF tandem mass spectrometer (Applied Biosystems, AB 4700). The PMF was obtained in a positive reflector mode using CHCA as matrix. 10 most intense peptides as well as few specific peptides for RFX5DBD which were identifiable from PMF were further analyzed by MSMS. The PMF and MSMS spectra were annotated by in-house MASCOT (Matrixscience, UK) database using GPS-Explorer software (v 3.6).

3. Results

3.1. Expression and purification of GST tagged RFX5DBD

The GST fusion recombinant protein was induced with IPTG and the protein was isolated and affinity purified on glutathione-Sepharose 4B beads. RFX5DBD was further purified to >95% homogeneity using superdex-75 size exclusion chromatography and was analyzed by SDS-PAGE. Fig. 2a shows SDS-PAGE of purified RFX5DBD. The identity of the protein was further verified using MALDI mass spectrometry (data not shown).

3.2. Electrophoretic mobility shift assay

The association of RFX5DBD and X-box DNA was verified by EMSA. Purified RFX5DBD was mixed with the oligonucleotide. Control experiment was performed with BSA. RFX5DBD strongly bound to the DNA (Fig. 2b, lane 2) and showed an up-shift of the band related to the protein DNA complex and the free probe left was negligible. On the other hand BSA showed no up-shift of the band regarding protein–DNA complex (Fig. 2b, lane 3). Thus the specificity of the RFX5DBD-X-box DNA complex was established.

3.3. Fluorescence study of the UV induced tyrosine cross linking at various pHs

Six tyrosine residues and a single tryptophan residue are present in the primary sequence of RFX5DBD. The protein when irradiated at 280 nm for 5 min the formation of dityrosine, a tyrosine modification in protein [16,17,21,25] was observed by fluorescence measurements of the sample using $\lambda_{ex} = 315$ nm [45] and $\lambda_{em} \sim 400$ nm. The newly formed fluorophore was further characterized at various pH and with reducing and non-reducing conditions in presence and absence of DTT [24,25]. Results showed increased DT formation in the protein under alkaline pH, at pH 11 (Fig. 3a) and in the absence of DTT. Fig. 3b shows a histogram representation of the intensities of DT fluorescence for the RFX5DBD at different alkaline pH, in presence and absence of DTT showing inhibition of DT formation above pH 7 in presence of 100 mM DTT. Addition of 100 mM DTT to RFX5DBD prior to UV irradiation almost completely prevented DT formation as DTT transfer electron to phenoxy radicals and convert tyrosyl radical to tyrosine. The protein after formation of DT in a buffer of pH 7.5 was also treated with 6 M GdmCl at 25 °C for 30 min and once again DT fluorescence was monitored to observe the effect of denaturation. A huge increase in the intensity of DT fluorescence was observed compared to the native protein at the same pH, which does not show any appreciable DT fluorescence (inset of Fig. 3a).

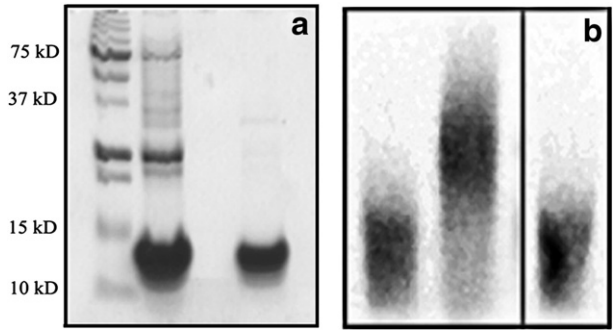

Fig. 2. (a) Coomassie-stained gel of purified RFX5DBD after SDS-PAGE. Lanes show: 1, molecular weight markers; 2, GST-cleaved RFX5DBD before gel filtration; 3, GST-cleaved RFX5DBD (12 kDa) after gel filtration. (b) Electromobility shift assay analyzed in a 6% non-denaturing polyacrylamide gel. Lanes show: 1, biotinylated free X-box DNA; 2, biotinylated X-box DNA in presence of 5 μM purified RFX5DBD and 3, biotinylated X-box DNA in presence of 5 μM BSA, taken from another experiment.

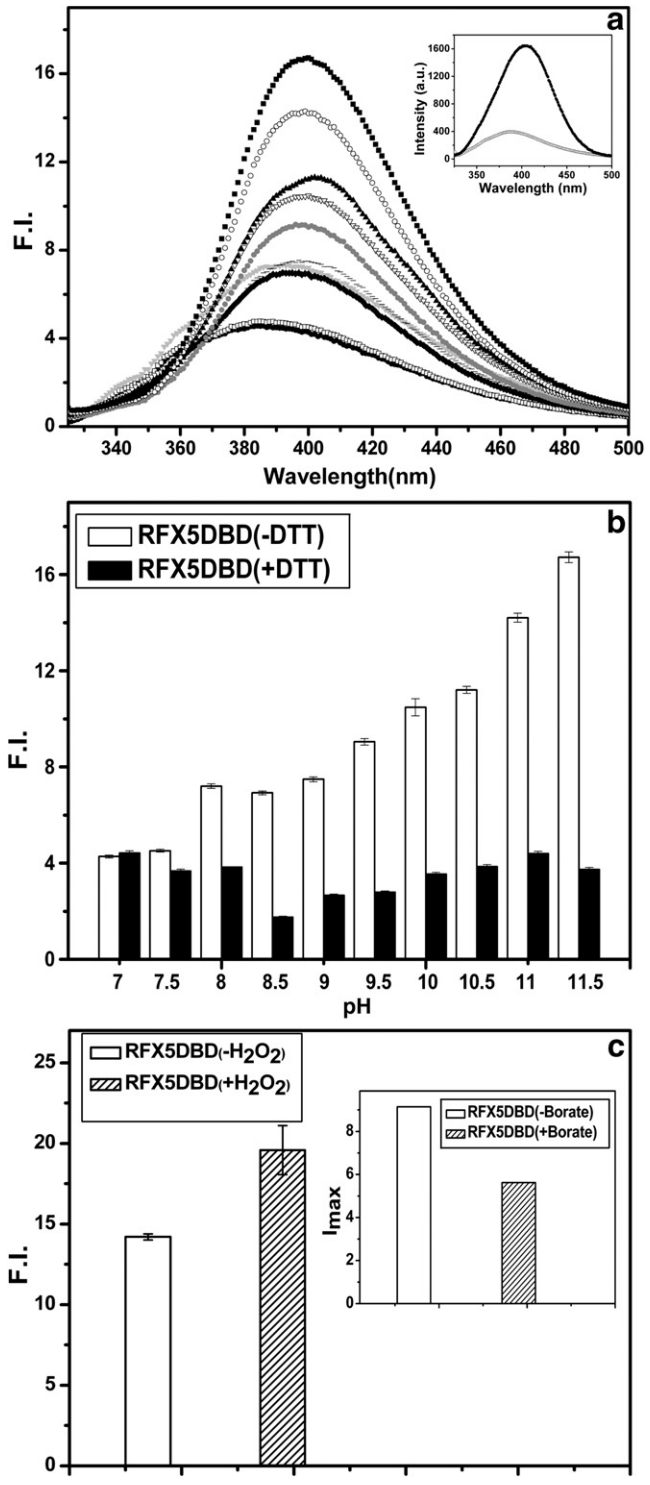

Fig. 3. (a) Emission spectra of DT formed in RFX5DBD at different pH upon excitation at 315 nm. The symbols represent (●) pH 7; (□) pH 7.5; (▼) pH 8; (♦) pH 8.5; (—) pH 9; (●) pH 9.5; (▽) pH 10; (▲) pH 10.5; (○) pH 11; (■) pH 11.5 all in the absence of 100 mM DTT. Inset of (a) shows the DT fluorescence emission in absence (○) and presence (●) of 6 M GdmCl at pH 7.5. (b) Histogram representation of fluorescence intensity of DT of RFX5DBD at 400 nm (Ex: −315 nm), in presence and absence of 100 mM DTT, with increasing pH. The error bars are SEM of four independent experiments. (c) Histogram representation of fluorescence intensity of DT derivative at 400 nm (Ex: −315 nm) of RFX5DBD in presence and absence of 1 mM H_2O_2 and HRP at pH 11. The error bars are SEM of four independent experiments. The inset shows the same of fluorescence intensity at λ_{max} in presence and absence of borate solution at pH 8.7 (Ex: −315 nm).

3.4. Effect of HRP/H_2O_2 and borate on tyrosine modification

Hydroxy radical generated from enzymatic action of HRP/H_2O_2 also triggers DT formation to a greater extent in RFX5DBD. The reduction potential of tyrosineO$^{\bullet}$/tyrosineOH couple is 0.88 V indicating the coupled reaction to be thermodynamically favorable [16]. H_2O_2 being a reactive oxygen species satisfies the criteria required for tyrosineO$^{\bullet}$ radical formation which is the precursor for DT. The ferric ion present in the heme protein horseradish peroxidase (HRP) participates in the electron transfer process and H_2O_2/peroxidase catalysis thus facilitates DT formation [24]. When RFX5DBD (0.03 mg/ml) was incubated with HRP (5 μg/ml) and 1 mM H_2O_2 for 30 min at 25 °C, intensity of DT emission increased 1.4 fold compared to that in the absence of H_2O_2/peroxidase at pH 11, shown in Fig. 3c. Incubation of RFX5DBD after DT formation, in 0.5 M borate/boric acid solution at pH 8.7, led to quenching of DT fluorescence along with a blue shift in the emission maxima to 387 nm from ~400 nm, shown in the inset of Fig. 3c.

3.5. Lifetime of DT in RFX5DBD

The decay profile of DT fluorophore in RFX5DBD was best fitted by two-exponentials with $\tau_c^1 = 1.726$ ns ($A_1 = 37.74\%$) and $\tau_c^2 = 5.187$ ns ($A_2 = 62.26\%$) associated with a χ^2 of 1.09. The mean lifetime was 3.88 ns.

3.6. Conformational alteration under alkaline condition

Far UV-CD spectra were recorded from 200 to 250 nm as shown in Fig. 4. The native RFX5DBD showed a minima at around 207 nm and a shoulder at around 218 nm at pH 7.5 (Fig. 4 (1)) indicating the presence of both α-helical and β-sheet structures. The magnitude of helicity estimated was 44% at pH 7.5 (using Eqs. (1)–(3)). At pH 11 the minima appeared at 204 nm and the shoulder at 219 nm (Fig. 4 (2)) associated with reduced helicity estimated to be 33% in RFX5DBD. The CD spectrum after treatment of HRP/H_2O_2 revealed the minima at around 206 nm and the shoulder at 222 nm (Fig. 4 (3)) showing little change in the helicity (34%) of RFX5DBD.

Again the analysis of the secondary structure of RFX5DBD with CDSSTR under different conditions is presented in Table 1. It shows that the total helicity (sum of alpha helix, 3/10 helix and PPr2) of RFX5DBD at pH 7.5 was estimated to be 32.6%.which is lesser as calculated using Eqs. (1)–(3). The sum of percentage of β sheet and turn is 28.7. The protein at pH 11 showed decreased total helicity (24%) with increased sum of β sheet and turn contribution (35.8%).

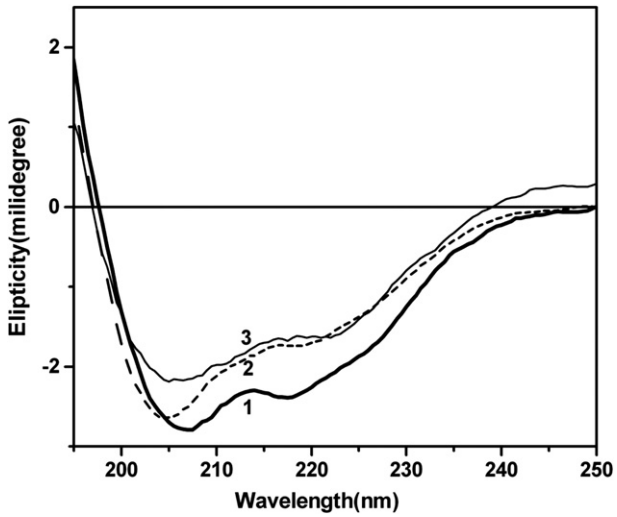

Fig. 4. Three representative far-UV CD spectra of 15 μM RFX5DBD at (1) pH 7.5, (2) pH 11 and (3) pH 11 pre-treated with HRP/H_2O_2.

Table 1
Quantitative analysis of the secondary structural content in RFX5DBD under different conditions using CDSSTR from CDPro with Basis set SP22X.

Sample	Helix	3/10 Helix	Sheet	Turn	PP2[a]	Unstructured	RMSD
RFX5DBD (pH 7.5)	17.1%	6.4%	16.4%	12.3%	9.1%	38.0%	0.099
RFX5DBD (pH 11)	7.4%	8.4%	22.5%	13.3%	8.2%	40.3%	0.135
RFX5DBD (pH 11, with HRP/H_2O_2)	6.7%	5.7%	23.6%	12.1%	9.0%	42.5%	0.132

[a] Poly(Pro)II structure.

RFX5DBD when treated with HRP/H_2O_2 at pH 11 also showed similar trends (Table 1) Thus in high alkaline pH the secondary structure of RFX5DBD was altered which in turn facilitated the formation of DT.

3.7. Enhanced DT formation in RFX5DBD in presence of X-box DNA

RFX5DBD was first incubated with equimolar mixture of double stranded X-box DNA at pHs 7.5 and 11. The complexes were exposed to UV irradiation and then the emission spectra were recorded. Interaction with the X-box DNA caused 35% and 30% quenching of fluorescence at pHs 7.5 and 11 respectively upon excitation at 280 nm (Fig 5a). On the other hand, DT fluorescence in presence of DNA increased significantly by 3.3 fold at pHs 7.5 and 1.6 fold at pH 11 with a small red shift in the emission spectrum (Fig 5b). The increased yield of DT fluorescence, more pronounced at pH 7.5, indicated that the stronger interaction of DNA in physiological condition favored DT formation in RFX5DBD.

3.8. Kinetics of DT formation

RFX5DBD when excited at 280 nm showed an exponential increase of emission intensity at 400 nm ($I_{400\,nm}$) and a pseudo first order kinetics of tyrosine dimerization in RFX5DBD was obeyed at 4 °C and pH 11, shown in Fig. 5c. The intensity profile reached saturation after ~4 min where as at pH 7.5 no appreciable increase in $I_{400\,nm}$ was observed and instead a decrease in fluorescence intensity was seen after ~2 min. The protein, pre-incubated with X-box DNA, when irradiated at 280 nm and pH 7.5, showed increased DT fluorescence. At pH 11 the presence of DNA also increased the rate of DT formation in RFX5DBD. Rate constants in absence and presence of DNA at pH 11 are $15.9\times10^{-3}\,s^{-1}$ and $21.6\times10^{-3}\,s^{-1}$ respectively as obtained from non-linear curve fitting analysis. Therefore, under normal condition DT is formed at high alkaline pH and no characteristic DT fluorescence was observed at pH 7.5. However DNA induced rapid formation of DT in RFX5DBD is facilitated at both pHs 7.5 and 11 as evidenced from the steady-state fluorescence and kinetic data (Fig. 5).

3.9. Homology model of RFX5DBD

The homology modeling program Modweb, a web interface for Modeller was used to predict the structure of RFX5DBD. The model was built for residue number 19 to 83 based on homology search. First few amino acids (11–18) were added to the rest of the model by Insight II and continuity of the first helix was maintained. The secondary structure of the model was analyzed by Ramachandran plot [46] which showed 41.1% helix and 34.2% β sheet like character (Supplementary material 1). Six tyrosine residues present in the protein are Y^{14}, Y^{16}, Y^{18}, Y^{39}, Y^{42} and Y^{45}. First three tyrosine residues are present in the first helix and are more surface exposed where the rest of the three residues are situated in the second helix and are present in the core of the protein. The spatial distribution of these tyrosine residues are shown in the model structure (Fig. 6). The closest pair of tyrosines are Y^{39} and Y^{42}. The closest distance between the ortho carbons of the two respective phenyl rings is 4.20 Å whereas

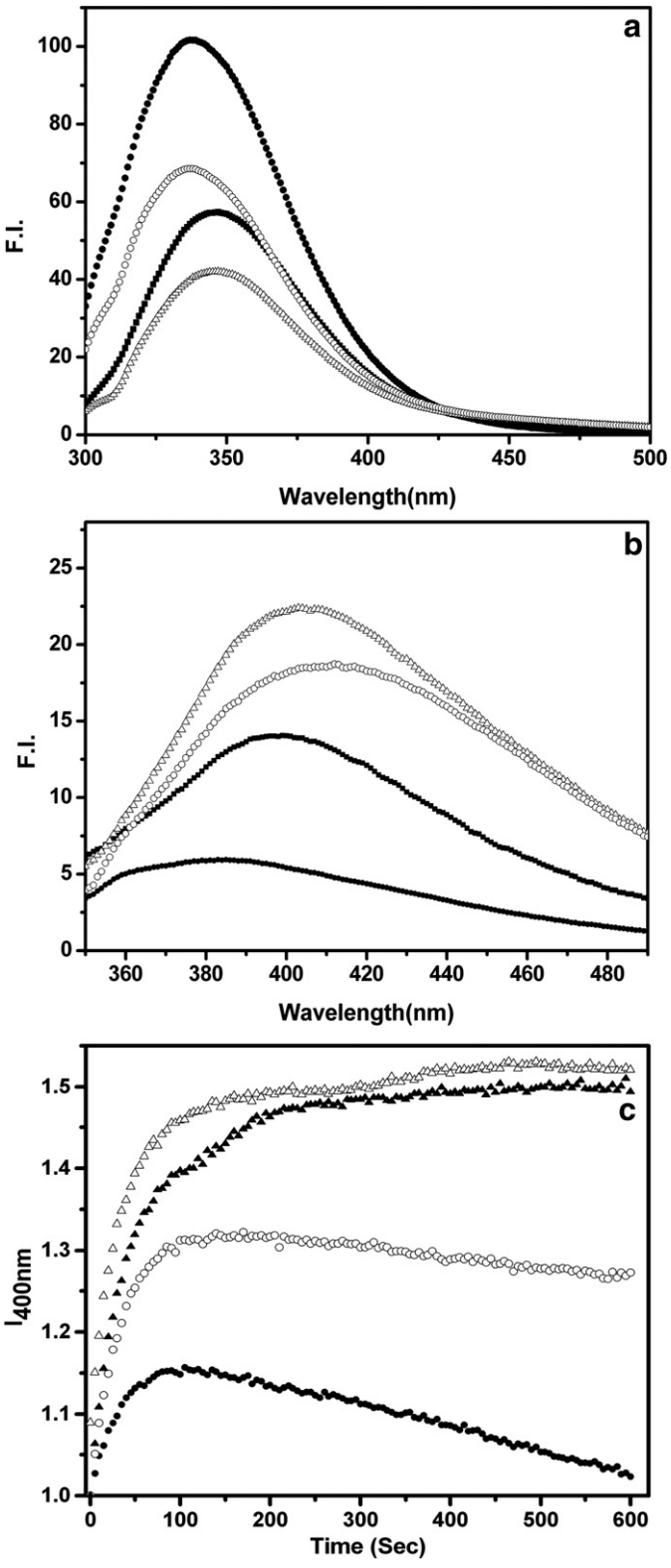

Fig. 5. Emission spectra of RFX5DBD in absence and presence of X-box DNA at two different pH. The symbol represents (■) at pH 11, in absence of DNA; (●) at pH 7.5, in absence of DNA; (△) at pH 11, in presence of DNA; (○) at pH 7.5, in presence of DNA. (a) Emission spectra upon excitation at 280 nm and (b) upon excitation at 315 nm. (c) Time dependent formation of DT in RFX5DBD, in absence and presence of X-box DNA are shown at 4 °C and two different pH when the emission intensity was measured at 400 nm (Ex: 280 nm). The symbols represent (●) pH 7.5, without DNA, (○) pH 7.5, with DNA, (▲) pH 11, without DNA and (△) pH 11, with DNA.

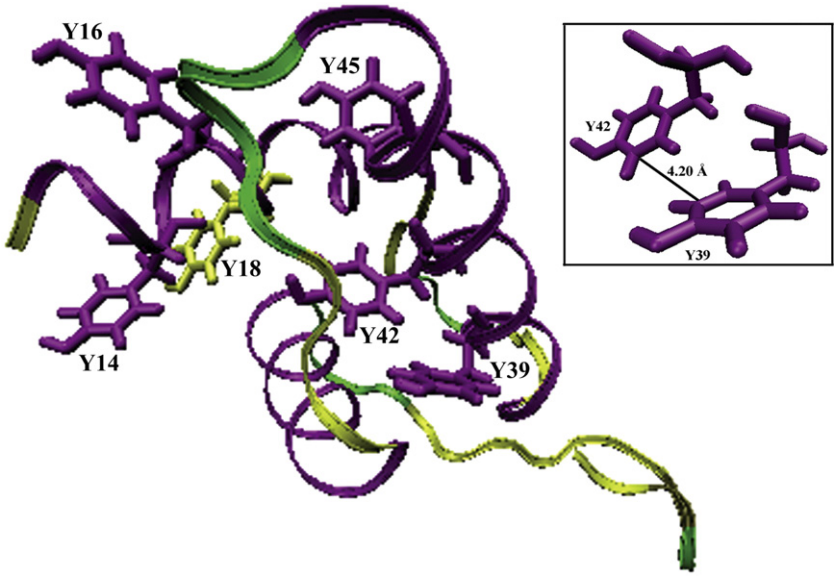

Fig. 6. Model of RFX5DBD (residue 11–83). Color denotes: purple for α-helix, green for turn and yellow for coil. Positions of six tyrosine residues are also shown in the model. Inset shows the distance between two ortho carbon atoms of the phenyl rings of Y^{39} and Y^{42}.

the same distance for Y^{42} and Y^{45} is 6.43 Å. Y^{14} and Y^{18} are present at the same side of the first helix and Y^{16} is at the opposite side and far apart from them. Another pair of tyrosines is Y^{14} and Y^{18} where the ortho carbons of the rings are 7 Å apart. Therefore we proposed that DT is formed between Y^{39} and Y^{42}.

3.10. UV protection of RFX5DBD by X-box DNA

Since reactive oxygen species is a potent destroyer for both protein and DNA, RFX5DBD was treated for 15 min with HRP and H_2O_2 followed by a more lethal dose of UV than applied before in previous experiments, with 254 nm UV lamp. Similar treatments were also made with RFX5DBD pre-incubated with DNA at 4 °C for 10 min. After treatment, samples were analyzed by 15% SDS-PAGE. Results showed that the band intensity around 12 kDa decreased due to UV exposure for 10 s and nearly disappeared when the UV exposure increased to 25 s (lanes 4 and 5 in inset of Fig. 7a). The presence of DNA increased the peroxidase/UV tolerance of RFX5DBD under similar conditions showing more intense bands in lanes 6 and 7 compared to those in lanes 4 and 5. Densitometry analysis also supports the protective role of DNA from degradation of RFX5DBD (not shown). The bands from the gel were digested with trypsin and analyzed by mass spectrometry. The resulting PMF spectrum of the untreated sample showed a peak at *m/z* 1609.29 (Fig. 7a) which was almost abolished when the protein was treated with UV radiation (Fig. 7b). After UV irradiation of RFX5DBD in presence of X-box DNA the peak at *m/z* 1609 reappeared together with an increase in intensity of the peak (Fig. 7c). This peptide fragment was further analyzed by MS/MS and the sequence obtained is NHLEEHTDTCLPK. This peptide was attributed to the region (N23–K35) of RFX5DBD. The sequence of hRFX5DBD when aligned using psi BLAST with the sequence of hRFX1DBD, with known crystal structure [47], this particular region of (N23–K35) showed sequence alignment with the region [7DNYETAEGVSLPR19] of hRFX1DBD (inset of Fig. 7c), assigned as a potential DNA binding site in RFX1DBD. Though we could only identify one protected peptide sequence, it still provides a direct evidence that the DNA binding cleft of RFX5DBD is protected by DNA from oxidative damage conferring more stability to the protein–DNA complex under UV exposure. This may have a correlation with the increased DT formed in RFX5DBD in presence of DNA as several previous works reported DT to provide conformational stability in structural proteins [48–50].

4. Discussions

Studies on the extent of oxidative damage by UV or ionizing radiation have been extensively done on DNA and not so much on proteins. However, it has been known that the oxidatively modified proteins could act as biomarkers of aging, neurodegenerative processes and cardiovascular diseases [51]. With the growing identification of oxidized proteins as pathophysiological marker, interest on DT cross linking in proteins has increased. DT is known to occur in many proteins like calmodulin [25], crystallins [24], skeletal muscle protein, myoglobin and hemoglobin [18] and in amyloid-β peptide in Alzheimer's disease [52] under oxidative stress, mimicked either by UV irradiation or by enzymatic action. The intramolecular DT formation in lac repressor affects its structure and its interaction with operator DNA as revealed by molecular modeling study by Gras et al. where conformational parameters of the protein are changed [53]. Similar work has been performed with lac repressor–operator system where effect of formation of DOPA on complex stabilization, H-bond network, electrostatic potential change was investigated by molecular dynamics simulation [54].

High abundance of tyrosine residues in RFX5DBD (6 Tyr) gave appreciable DT fluorescence when subjected to oxidative cross linking of tyrosine residues. The mean lifetime of DT in RFX5DBD was 3.88 ns which matched well with the mean lifetime of 4.3 ns for free synthetic DT [39]. Also the maxima of bimodal lifetime distribution of dityrosine in yeast spore wall centered at $\tau_c^1 = 0.5$ ns and $\tau_c^2 = 2.6$ ns [55]. The DT derivatives formed in RFX5DBD are of intramolecular type as no higher molecular weight cross-linked products were observed in SDS-PAGE under our experimental conditions.

Fig. 7. Peptide mass finger print (PMF) of RFX5DBD (a) Before UV irradiation; (b) After UV irradiation; (c) After UV irradiation of the protein pre-incubated with equimolar X-box DNA. The inset of (a) shows 15% SDS-PAGE where RFX5DBD was treated with peroxidase/UV exposure in presence and absence of X-box DNA and are run in the gel. Lanes show: 1, molecular weight marker; 2 and 3; untreated RFX5DBD in absence and presence of X-box DNA; 4 and 5; 10 s and 25 s UV exposure to RFX5DBD in absence of X-box DNA respectively; 6 and 7; similar for lanes 4 and 5 except in presence of X-box DNA. Inset of (c) shows the alignment of hRFX5DBD with hRFX1DBD. The identical residues are mentioned with letters and positive sign indicates similar residues. Analysis of the alignment data shows 33% identity and 60% similarity in these two sequences. The box drawn in the sequences represent the one in the DNA binding region of hRFX1.

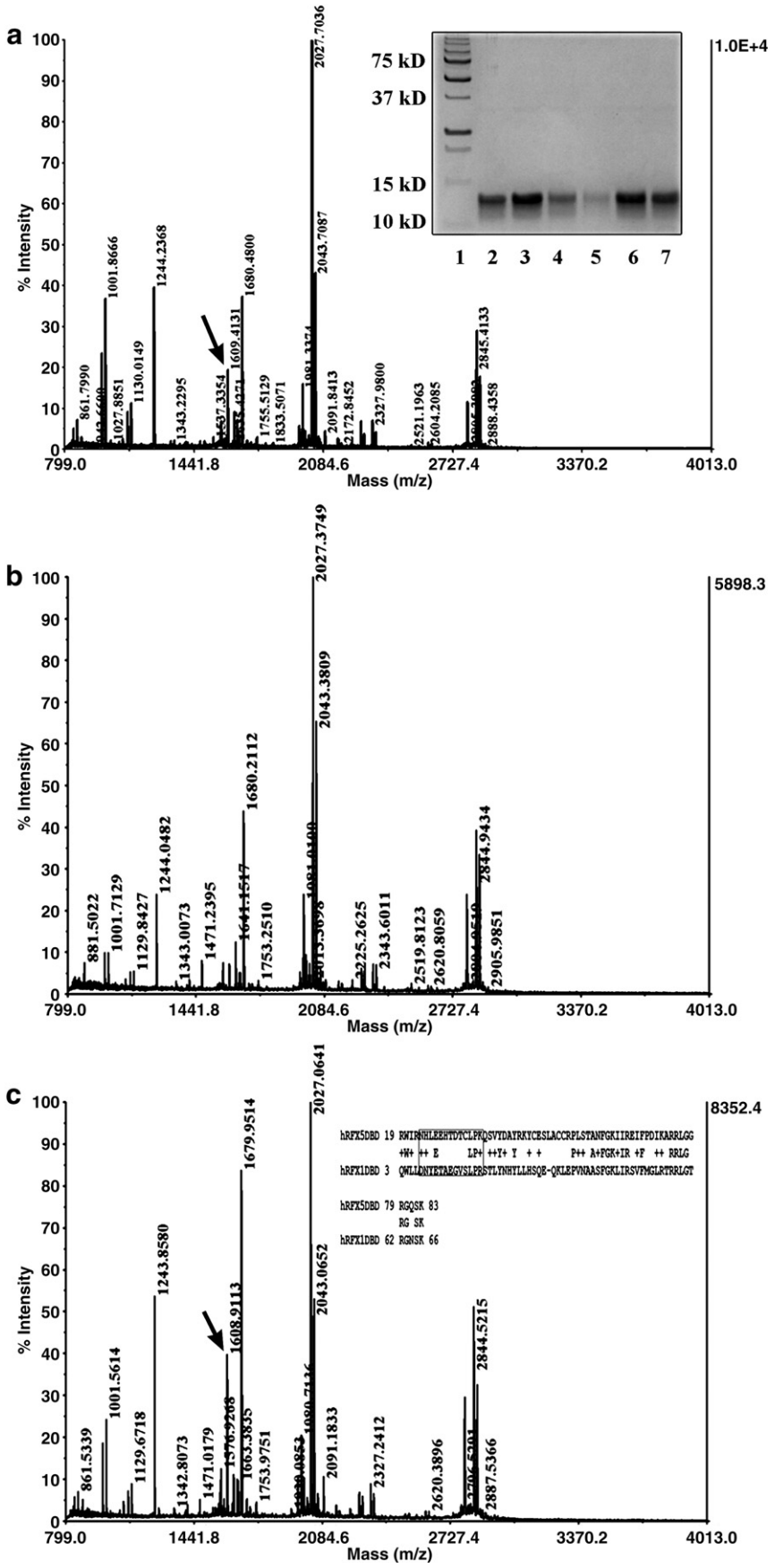
a
1.0E+4
75 kD
37 kD
15 kD
10 kD
1 2 3 4 5 6 7
% Intensity
Mass (m/z)
799.0
1441.8
2084.6
2727.4
3370.2
4013.0
b
5898.3
c
8352.4
hRFX5DBD 19 RWIPNHLEEHTDTCLPFQSVYDAYRYCESLACCRPLSTANFGKIIREIFPDIKARRLGG
hRFX1DBD 3 QWLLDNYETAEGYSLPRSTLYNHYLLHSQE-QKLEPVNAASFGKLIRSVFMGLRTRRLGT
hRFX5DBD 79 RGQSK 83
hRFX1DBD 62 RGNSK 66

Modeling data suggested that the most susceptible tyrosine residues involved in DT formation are Y^{39} and Y^{42}. They are the closest pair of tyrosine where ortho carbons of the rings are separated by 4.20 Å. This observation is further supported by the fact that when DT formed protein was unfolded with 6 M GdmCl the intensity of DT fluorescence increased implying the core tyrosine to be engaged in DT formation. Moreover DT fluorescence increases in presence of DNA. Not only the fluorescence intensity of DT was enhanced at pH 11 even at physiological pH of 7.5 the presence of DNA facilitated formation of DT in the protein (Fig. 5b). These were also reflected in the kinetic data. RFX5DBD when irradiated at 280 nm, at pH 11, the intensity of DT fluorescence increased exponentially with time and approached a saturation value within 250 s, comparable with the kinetics of DT formation in calmodulin, in presence or absence of Ca^{+2} approaching saturation within about 4 min [25]. At pH 11 the rate constant of DT formation in RFX5DBD was faster ($21.6\times10^{-3}\,s^{-1}$) in presence of DNA than in absence of it ($15.9\times10^{-3}\,s^{-1}$).

Sequence homology between hRFX1DBD and hRFX5DBD revealed that one of the DNA binding residues R^{19} of hRFX1DBD, obtained from the crystal structure of RFX1DBD in complex with DNA, [47] is aligned with K^{35} of hRFX5DBD a positively charged amino acid residue like R. Therefore it is easily understandable that K^{35} of hRFX5DBD is involved in direct or water mediated DNA contact like R^{19} of hRFX1DBD–DNA complex if the secondary structure of RFX5DBD in free or bound state is not altered very much as the template for our model is in bound conformation. CD spectral analysis of RFX5DBD in presence or absence of DNA showed no significant secondary structure alteration (data not shown). However there is example like lac repressor where DNA binding induces the formation of a helix in the hinge region of the protein which remains disordered in the free state [56]. In RFX5DBD the closest distance between K^{35} and ring carbon of Y^{39} as proposed from the model is 5.21 Å that that means these two residues are in close vicinity of each other. Therefore we proposed that when DNA makes contact with K^{35} that alters the position of the side chain residues of other amino acids of that core region of RFX5DBD. Even a minor alteration of the side chains could result Y^{39} and Y^{42} to be more close to each other and could result in more flexible DT formation between them.

Analysis of CD spectra using Eqs. (1)–(3) revealed 44% helical content in RFX5DBD at pH 7.5 which is in well agreement with the extent of helicity analyzed by Ramachandran plot (41% helix) presented in Supplementary material 1. On the other hand results from analysis using CDSSTR showed 33% total helicity and 29% total β structure. Ramachandran plot, also showed comparable β structure (34%). Using both the methods we found that the CD spectral feature of RFX5DBD was altered at alkaline pH of 11 and showed lesser helical content, from 44% to 33% using Eqs. (1)–(3) and 33% to 24% using CDSSTR. The DT formation in presence of peroxidase/H_2O_2 increased the quantum yield of DT with little change in helical content (Figs. 3c and 4). Along with it we also found the β sheet content to increase at alkaline pH (Table 1). Therefore, it indicates the conformational change induced by the formation of DT in RFX5DBD. It was reported in literature that intra-molecular ditryptophan has the potential to induce and stabilize antiparallel β-strands in short peptides and in global respect in the local peptide structure in proteins. Dityrosine, another naturally occurring biaryl cross link in proteins could also stimulate structural alteration and could give stability in antiparallel β-strands [57] and we also found increased β character in the protein under condition of DT formed. In calmodulin the level of α-helical structure is also reduced upon DT cross linking. On the other hand the CD spectra of bovine pancreatic ribonuclease A (RNase A) and γB-crystallin are not changed significantly when DT cross links are present [58].

The DNA bound RFX5DBD when subjected to oxidative stress shows two important observations regarding the protein stability and conformation. First of all the quantum yield of DT in RFX5DBD increased significantly upon association with X-box DNA as already discussed. The second significant finding results in the protection of RFX5DBD by the DNA partner from UV degradation. The bare protein, when exposed to peroxide/UV at a still higher dose than required for DT formation, led to degradation of RFX5DBD. However, in presence of DNA the protein is stabilized (inset of Fig. 7a). Similar result was obtained when the DNA binding chromosomal protein MC1 was irradiated in complexation with DNA, the binding site of MC1 was found protected by the bound DNA [59]. The mass spectrometry data clearly revealed that one of the peptides (m/z 1609) in RFX5DBD was being protected from oxidation in presence of DNA. The sequence of hRFX5DBD when aligned to hRFX1DBD (The inset of Fig. 7c), this particular peptide sequence was found to align in the region of RFX1 where one of the DNA binding residues (R^{19}) was present. A similar residue in RFX5DBD is K^{35} again the similar residue near of which DT is formed. This result reinforces the correlation between the UV protection of RFX5DBD by DNA and DT formation in it. We hypothesized that DT formation in RFX5DBD gave structural stability, more in presence of the DNA and tyrosines are exposed to oxidation and prevent the DNA binding core to be oxidized and degraded. UV irradiation causes zero length covalent cross linking between protein and nucleic acid and those amino acids which are present in the DNA binding sites are cross linked to the nucleobases [60]. However, we did not observe any cross linked product in the SDS-PAGE probably due to its lower abundance.

These results implied that RFX5DBD formed intra-molecular DT under exposure of UV and became more stable when associated with DNA exhibiting stronger DT fluorescence. The DNA binding proteins generally protect DNA molecule from the external stress mediated by $OH^{\bullet}$ or UV exposure to maintain the biological function of the DNA and themselves get modified [8]. On the other hand there is a protection due to the masking of the binding site of the protein by DNA [59]. The presence of intra-molecular DT in RFX5DBD results in conformational alteration inducing cross-protection in both DNA and the protein in their complex under oxidative stress.

Appendix A. Supplementary data

Supplementary data associated with this article can be found, in the online version, at doi:10.1016/j.bpc.2010.04.005.

References

[1] K.J. Davies, M.E. Delsignore, S.W. Lin, Protein damage and degradation by oxygen radicals. II. Modification of amino acids, J. Biol. Chem. 262 (1987) 9902–9907.
[2] T. Grune, P. Michel, N. Sitte, W. Eggert, H. Albrecht-Nebe, H. Esterbauer, W.G. Siems, Increased levels of 4-hydroxynonenal modified proteins in plasma of children with autoimmune diseases, Free Radic. Biol. Med. 23 (1997) 357–360.
[3] H.P. Ciolino, R.L. Levine, Modification of proteins in endothelial cell death during oxidative stress, Free Radic. Biol. Med. 22 (1997) 1277–1282.
[4] A. Zaidi, M.L. Michaels, Effects of reactive oxygen species on brain synaptic plasma membrane Ca^{2+}-ATPase, Free Radic. Biol. Med. 27 (1999) 810–821.
[5] E.R. Stadtman, Covalent modification reactions are marking steps in protein turnover, Biochemistry 29 (1990) 6323–6331.
[6] E.R. Stadtman, Oxidation of free amino acids and amino acid residues in proteins by radiolysis and by metal-catalyzed reactions, Ann. Rev. Biochem. 62 (1993) 797–821.
[7] B.S. Berlett, E.R. Stadtman, Protein oxidation in aging, disease, and oxidative stress, J. Biol. Chem. 272 (1997) 20313–20316.
[8] N. Gillard, S. Goffinont, C. Bure, M. Davidkova, J.C. Maurizot, M. Cadene, M. Spotheim-Marizot, Radiation-induced oxidative damage to the DNA-binding domain of the lactose repressor, Biochem. J. 403 (2007) 463–472.
[9] T. Okajima, Y. Kawata, K. Hamaguchi, Chemical modification of tryptophan residues and stability changes in proteins, Biochemistry 29 (1990) 9168–9175.
[10] S. Vazquez, J.A. Aquilina, J.F. Jamie, M.M. Sheil, R.J. Truscott, Novel protein modification by kynurenine in human lenses, J. Biol. Chem. 277 (2002) 4867–4873.
[11] Y. Fukunaga, Y. Katsuragi, T. Izumi, F. Sakiyama, Fluorescence characteristics of kynurenine and N′-formylkynurenine. Their use as reporters of the environment of tryptophan 62 in hen egg-white lysozyme, J. Biochem. 92 (1982) 129–141.
[12] G. Boguta, A.M. Dancewicz, Radiolytic and enzymatic dimerization of tyrosyl residues in insulin, ribonuclease, papain and collagen, Int. J. Radiat. Biol. 43 (1983) 249–265.
[13] L.R. Karam, M. Dizdaroglu, M.G. Simic, OH radicalinduced products of tyrosine peptides, Int. J. Radiat. Biol. 46 (1984) 715–724.
[14] K.J. Davies, Protein damage and degradation by oxygen radicals. I. General aspects, J. Biol. Chem. 262 (1987) 9895–9901.

[15] C. Giulivi, K.J. Davies, Dityrosine: a marker for oxidatively modified proteins and selective proteolysis, Methods Enzymol. 233 (1994) 363–371.
[16] C. Giulivi, N.J. Traaseth, K.J. Davies, Tyrosine oxidation products: analysis and biological relevance, Amino Acids 25 (2003) 227–232.
[17] D.A. Malencik, S.R. Anderson, Dityrosine as a product of oxidative stress and fluorescent probe, Amino Acids 25 (2003) 233–247.
[18] C. Giulivi, K.J. Davies, Mechanism of the formation and proteolytic release of H2O2-induced dityrosine and tyrosine oxidation products in hemoglobin and red blood cells, J. Biol. Chem. 276 (2001) 24129–24136.
[19] B. Gmeiner, C. Seelos, Phosphorylation of tyrosine prevents dityrosine formation in vitro, FEBS Lett. 255 (1989) 395–397.
[20] R. Aeschbach, R. Amadò, H. Neukom, Formation of dityrosine cross-links in proteins by oxidation of tyrosine residues, Biochim. Biophys. Acta 439 (1976) 292–301.
[21] D.A. Malencik, S.R. Anderson, Dityrosine formation in calmodulin: conditions for intermolecular cross-linking, Biochemistry 33 (1994) 13363–13372.
[22] G.J. Smith, The fluorescence of dihydroxyphenylalanine: the effects of protonation–deprotonation, Coloration Technol. 115 (1999) 346–349.
[23] T.G. Huggins, M.C. Wells-Knecht, N.A. Detorie, J.W. Baynes, S.R. Thorpe, Formation of o-tyrosine and dityrosine in proteins during radiolytic and metal-catalyzed oxidation, J. Biol. Chem. 268 (1993) 12341–12347.
[24] P. Guptasarma, D. Balasubramanian, Dityrosine formation in the proteins of the eye lens, Curr. Eye Res. 11 (1992) 1121–1125.
[25] D.A. Malencik, S.R. Anderson, Dityrosine formation in calmodulin, Biochemistry 26 (1987) 695–704.
[26] K. Masternak, E. Barras, M. Zufferey, B. Conrad, G. Corthals, R. Aebersold, J.C. Sanchez, D.F. Hochstrasser, B. Mach, W. Reith, A gene encoding a novel RFX-associated transactivator is mutated in the majority of MHC class II deficiency patients, Nat. Genet. 20 (1998) 273–277.
[27] U.M. Nagarajan, P. Louis-Plence, A. DeSandro, R. Nilsen, A. Bushey, J.M. Boss, RFX-B is the gene responsible for the most common cause of the bare lymphocyte syndrome, an MHC class II immunodeficiency, Immunity 10 (1999) 153–162.
[28] V. Steimle, B. Durand, E. Barras, M. Zufferey, M.R. Hadam, B. Mach, W. Reith, A novel DNA-binding regulatory factor is mutated in primary MHC class II deficiency (bare lymphocyte syndrome), Genes Dev. 9 (1995) 1021–1032.
[29] B. Durand, P. Sperisen, P. Emery, E. Barras, M. Zufferey, B. Mach, W. Reith, RFXAP, a novel subunit of the RFX DNA binding complex is mutated in MHC class II deficiency, EMBO J. 16 (1997) 1045–1055.
[30] B. Durand, M. Kobr, W. Reith, B. Mach, Functional complementation of major histocompatibility complex class II regulatory mutants by the purified X-box-binding protein RFX, Mol. Cell. Biol. 14 (1994) 6839–6847.
[31] W. Reith, S. Satola, C.H. Sanchez, I. Amaldi, B. Lisowska-Grospierre, C. Griscelli, M.R. Hadam, B. Mach, Congenital immunodeficiency with a regulatory defect in MHC class II gene expression lacks a specific HLA-DR promoter binding protein, RF-X, Cell 53 (1988) 897–906.
[32] C.S. Moreno, P. Emery, J.E. West, B. Durand, W. Reith, B. Mach, J.M. Boss, Purified X2 binding protein (X2BP) cooperatively binds the class II MHC X box region in the presence of purified RFX, the X box factor deficient in the bare lymphocyte syndrome, J. Immunol. 155 (1995) 4313–4321.
[33] R. Mantovani, The molecular biology of the CCAAT-binding factor NF-Y, Gene 239 (1999) 15–27.
[34] V. Steimle, L.A. Otten, M. Zufferey, B. Mach, Complementation cloning of an MHC class II transactivator mutated in hereditary MHC class II deficiency (or bare lymphocyte syndrome), Cell 75 (1993) 135–146.
[35] B. Mach, V. Steimle, E. Martinez-Soria, W. Reith, Regulation of MHC class II genes: lessons from a disease, Annu. Rev. Immunol. 14 (1996) 301–331.
[36] P. Emery, B. Durand, B. Mach, W. Reith, RFX proteins, a novel family of DNA binding proteins conserved in the eukaryotic kingdom, Nucleic Acids Res. 24 (1996) 803–807.
[37] O. Harari, J.K. Liao, Inhibition of MHC II gene transcription by nitric oxide and antioxidants, Curr. Pharm. Des. 10 (2004) 893–898.
[38] J.L. Duh, H. Zhu, H.G. Shertzer, D.W. Nebert, A. Puga, The Y-box motif mediates redox-dependent transcriptional activation in mouse cells, J. Biol. Chem. 270 (1995) 30499–30507.
[39] D.A. Malencik, S.R. Anderson, Fluorometric characterization of dityrosine: complex formation with boric acid and borate ion, Biochem. Biophys. Res. Commun. 178 (1991) 60–67.
[40] A. Gayen, C. Chatterjee, C. Mukhopadhyay, GM1-induced structural changes of bovine serum albumin after chemical and thermal disruption of the secondary structure: a spectroscopic comparison, Biomacromolecules 9 (2008) 974–983.
[41] E. Haque, D. Debnath, S. Basak, A. Chakrabarti, Structural changes of horseradish peroxidase in presence of low concentrations of urea, Eur. J. Biochem. 259 (1999) 269–274.
[42] S. Ray, M. Bhattacharyya, A. Chakrabarti, Conformational study of spectrin in presence of submolar concentrations of denaturants, J. Fluoresc. 15 (2005) 61–70.
[43] C.D. Schwieters, G.M. Clore, The VMD-XPLOR visualization package for NMR structure refinement, J. Magn. Reson. 149 (2001) 239–244.
[44] D. Bhattacharya, D. Mukhopadhyay, A. Chakrabarti, Hemoglobin depletion from red cell cytosol reveals new proteins in 2D gel based proteomics study, Proteomics Clin. App. 1 (2007) 561–564.
[45] G.S. Bayse, A.W. Michaels, M. Morrison, The peroxidase-catalyzed oxidation of tyrosine, Biochim. Biophys. Acta 284 (1972) 34–42.
[46] G.N. Ramachandran, C. Ramakrishnan, V. Sasisekharan, Stereochemistry of polypeptide chain configurations, J. Mol. Biol. 7 (1963) 95–99.
[47] K.S. Gajiwala, H. Chen, F. Cornille, B.P. Roques, W. Reith, B. Mach, S.K. Burley, Structure of the winged-helix protein hRFX1 reveals a new mode of DNA binding, Nature 403 (2000) 916–921.
[48] D.J. Raven, C. Earland, M. Little, Occurrence of dityrosine in Tussah silk fibroin and keratin, Biochim. Biophys. Acta 251 (1971) 96–99.
[49] J.W. Downie, F.S. Labella, M. West, An insoluble, dityrosine-containing protein from uterus, Biochim. Biophys. Acta 263 (1972) 604–609.
[50] K. Ramalingam, Chemical nature of monogenean sclerites. I. Stabilization of clamp-protein by formation of dityrosine, Parasitology 66 (1973) 1–7.
[51] S. Fu, M.J. Davies, R. Stocker, R.T. Dean, Evidence for roles of radicals in protein oxidation in advanced human atherosclerotic plaque, Biochem. J. 333 (1998) 519–525.
[52] D.P. Smith, G.D. Ciccotosto, D.J. Tew, M.T. Fodero-Tavoletti, T. Johanssen, C.L. Masters, K.J. Barnham, R. Cappai, Concentration dependent Cu^{2+} induced aggregation and dityrosine formation of the Alzheimer's disease amyloid-beta peptide, Biochemistry 46 (2007) 2881–2891.
[53] J. Gras, D. Sy, S. Eon, M. Charlier, M. Spotheim-Maurizot, Consequences of intramolecular dityrosine formation on a DNA–protein complex: a molecular modeling study, Radiat. Phys. Chem. 72 (2005) 271–278.
[54] S. Aci-Sèche, N. Garnier, S. Goffinont, D. Genest, M. Spotheim-Maurizot and M. Genest, Comparing native and irradiated *E. coli* lactose repressor–operator complex by molecular dynamics simulation, Eur. Biophys. J. in press, doi: 10.1007/s00249-010-0591-1.
[55] A.J. Kungl, A.J. Visser, H.F. Kauffmann, M. Breitenbach, Time-resolved fluorescence studies of dityrosine in the outer layer of intact yeast ascospores, Biophys. J. 67 (1994) 309–317.
[56] C.A. Spronk, M. Slijper, J.H. van Boom, R. Kaptein, R. Boelens, Formation of the hinge helix in the lac repressor is induced upon binding to the lac operator, Nat. Struct. Biol. 11 (1996) 916–919.
[57] J. Matthews, T. Dinh, P. Tivitmahaisoon, J. Ziller, D. Van Vranken, Intramolecular ditryptophan crosslinks enforce two types of antiparallel β structures, Chem. Biol. 8 (2001) 1071–1079.
[58] R. Kanwar, D. Balasubramanian, Structural studies on some dityrosine-cross-linked globular proteins: stability is weakened, but activity is not abolished, Biochemistry 39 (2000) 14976–14983.
[59] F. Culard, A. Gervais, G. de Vuyst, M. Spotheim-Maurizot, M. Charlier, Response of a DNA-binding protein to radiation-induced oxidative stress, J. Mol. Biol. 328 (2003) 1185–1195.
[60] H. Steen, J. Petersen, M. Mann, O.N. Jensen, Mass spectrometric analysis of a UV-cross-linked protein–DNA complex: tryptophans 54 and 88 of *E. coli* SSB cross-link to DNA, Protein Sci. 10 (2001) 1989–2001.